

# Spatial Wavefunctions of Spin

T. Peter Rakitzis

*Department of Physics, University of Crete, 70013 Heraklion-Crete, Greece*

*IESL-FORTH, N. Plastira 100, Heraklion-Crete 71110, Greece*

*Email: [ptr@iesl.forth.gr](mailto:ptr@iesl.forth.gr)*

We present an alternative formulation of quantum mechanical angular momentum, based on spatial wavefunctions that depend on the Euler angles  $\varphi, \theta, \chi$ . The wavefunctions are Wigner D-functions,  $D_{nM}^S(\varphi, \theta, \chi)$ , for which the body-fixed projection quantum number  $n$  has the unusual value  $n = |\mathbf{S}| = \sqrt{S(S+1)}$ , or  $n = 0$ . We show that the states  $D_{\sqrt{S(S+1)}M}^S(\varphi, \theta, \chi)$  of elementary particles with spin  $S$  give a gyromagnetic ratio of  $g = 2$  for  $S > 0$ , and we identify these as the spatial angular-momentum wavefunctions of known fundamental charged particles with spin. All known Standard-Model particles can be categorized with either value  $n = \sqrt{S(S+1)}$  or  $n = 0$ . Therefore, we make the case that the  $D_{nm}^j(\varphi, \theta, \chi)$  are useful as spatial wavefunctions for spin. The  $D_{nm}^j(\varphi, \theta, \chi)$  agree with all known angular momentum results. Some implications and new predictions related to the quantum number  $n$  for fundamental particles are discussed, such as the proposed Dirac-fermion nature of the neutrino, and some proposed dark-matter candidates.

## I. INTRODUCTION

In conventional quantum-mechanical angular-momentum theory, there are spatial wavefunctions for describing the angular position of an orbiting particle in a central field, the spherical harmonics  $Y_m^l(\theta, \varphi)$  (where  $l$  is the angular momentum quantum number, and  $m$  is the azimuthal quantum number, the projection of the angular momentum  $\mathbf{l}$  along the space-fixed  $Z$  axis). The  $Y_m^l(\theta, \varphi)$  give the probability amplitude of finding the particle at the angular location described by the angles  $\theta$  and  $\varphi$ . However, no analogous spatial wavefunction exists for angular momentum or spin in conventional quantum mechanics, which would describe the angular distribution of the angular momentum in terms of spatial coordinates. In fact, there is a deep-seated preconception in the physics community that spatial wavefunctions for spin do not exist (without proof). For example, in a well-known textbook [1] it is stated that: "... the electron also carries another form of angular momentum, which has nothing to do with motion in space (and which is not, therefore, described by any function of the position variables  $r, \theta, \varphi$ ) but which is somewhat analogous to classical spin (and for which, therefore, we use the same word)."

For the description of the rotation of bodies with internal structure (such as molecules), the Wigner  $D_{m' m}^j(\varphi, \theta, \chi)$  functions are spatial wavefunctions that describe the angular distribution of the body-fixed  $z'$  axis (which is parallel to the principle axis of the molecule) for given projections  $m$  and  $m'$  of  $j$  along  $Z$  and  $z'$ , respectively, and  $\varphi, \theta, \chi$  are the Euler angles. For the  $D_{m' m}^j(\varphi, \theta, \chi)$  to be non-divergent and normalizable  $m$  and  $m'$  must range from  $-j$  to  $+j$  in integer steps. We give three examples of using  $D_{m' m}^j(\varphi, \theta, \chi)$  as spatial wavefunctions, culminating in a proposal for a spatial wavefunction for the angular momentum vector  $\mathbf{j}$ .

First, we consider a symmetric-top molecule (such as  $\text{CH}_3\text{Cl}$ ) in the state  $|JKM\rangle \equiv D_{KM}^J(\varphi, \theta, \chi)$ , shown in Fig. 1 using the Vector Model.  $|D_{KM}^J(\varphi, \theta, \chi)|^2$  gives the probability of finding the principle axis of the molecule (the  $z'$  axis, parallel to the C-Cl bond and also the electric dipole moment of the molecule) at angle  $\theta$  to the  $Z$  axis. The expectation value of  $\cos\theta$  is given by  $\langle \cos\theta \rangle = KM/J(J+1)$ , so that selection of positive or negative values of  $KM$  will preferentially orient the

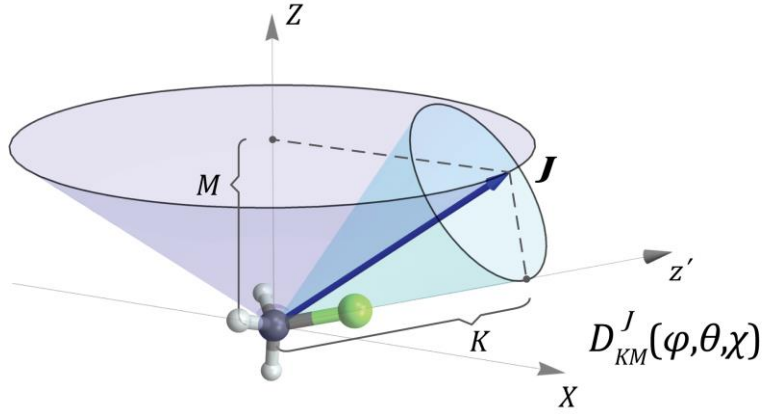


*Figure 1:* Vector-Model representation of the symmetric top molecule  $\text{CH}_3\text{Cl}$  in the  $|JKM\rangle$  state. The angular momentum  $\mathbf{J}$  projects  $M$  along the space-fixed  $Z$  axis, and  $K$  along the body-fixed  $z'$  axis (which is parallel to the principle axis of the molecule).

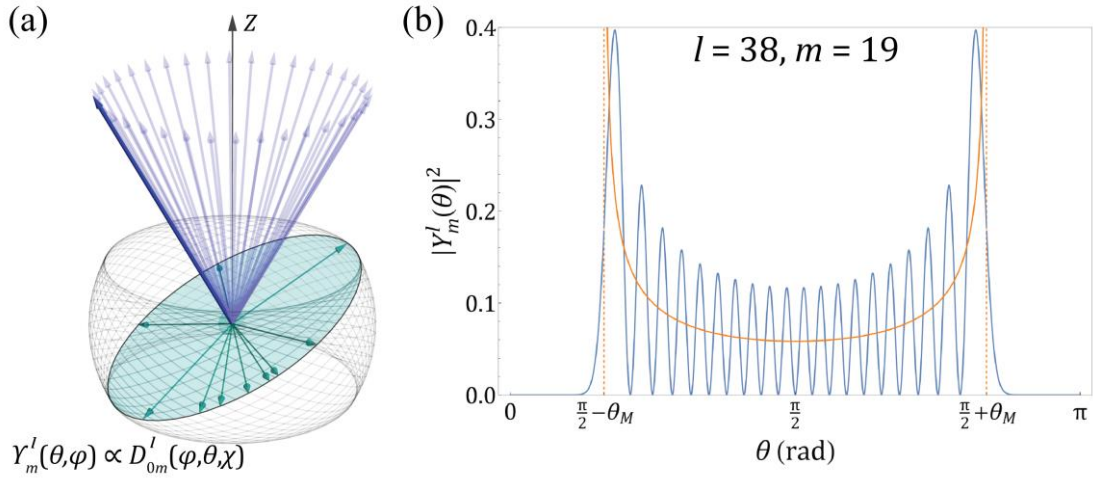


**Figure 2:** (a) Vector-Model description of the the  $Y_m^l(\theta, \varphi)$  state: the orbital angular momentum vector  $\mathbf{l}$  projects  $m$  along  $Z$ , and is delocalized around  $Z$  in a cone;  $\mathbf{l}$  also projects  $0$  along  $z'$  (which is parallel to the position of the particle  $\mathbf{r}$ ) and is perpendicular to the orbital plane of the orbiting particle (which precesses along with  $\mathbf{l}$ ). (b) Exact values of  $|Y_m^l(\theta, \varphi)|^2$  (in blue) are compared to the classical VM prediction of the probability distribution of the particle; the  $Y_m^l(\theta, \varphi)$  oscillate within the classically-allowed region, and decay exponentially outside it.

molecular principle axis parallel or antiparallel to the laboratory  $Z$  axis. Such  $|JKM\rangle$  state selection has been used to study the dependence of photodissociation and bimolecular reactions on the orientation and alignment of symmetric-top molecules [2,3,4,5,6,7,8].

Second, the  $Y_m^l(\theta, \varphi)$  spatial wavefunctions of orbital angular momentum are proportional to  $D_{0m}^j(\varphi, \theta, \chi)$ , with  $0$  projection of  $\mathbf{l}$  along the  $z'$  axis (as  $m' = 0$ ), so that  $\mathbf{l}$  is always perpendicular to  $z'$ . Therefore,  $z'$  is parallel to the position of the orbiting particle, and perpendicular to the orbital plane, as shown in Fig. 2a, using the Vector Model. This Vector-Model picture correctly shows that, asymptotically, the  $Y_m^l(\theta, \varphi)$  and the probability of finding the particle will only have nonzero values within the classically-allowed angle ranges of  $\frac{\pi}{2} - \theta_m \leq \theta \leq \frac{\pi}{2} + \theta_m$ , where  $\theta_m$  is the Vector-Model angle between  $\mathbf{l}$  and the  $Z$  axis, given by  $\cos\theta_m = m/|\mathbf{l}|$ . For finite values of  $l$ , the  $Y_m^l(\theta, \varphi)$  will oscillate within this classically-allowed region, and will decay exponentially outside this region, in the classically-forbidden region, as shown in Fig. 2b.

Finally, for the third example, we will consider something new: choosing the projection  $n$  in  $D_{nm}^j(\varphi, \theta, \chi)$  so that  $z'$  is parallel to the angular momentum  $\mathbf{j}$ , as shown in Fig. 3, using the Vector Model. In this case, we introduce a special angular momentum frame (the  $\mathbf{j}$  frame), which is unusual because all three components of  $\mathbf{j}$  are defined in this frame (here, the projection along  $z'$  is  $n = |\mathbf{j}| = \sqrt{j(j+1)}$ , and the projections along  $x'$  and  $y'$  are both  $0$ , by definition). At first sight, this choice may seem to violate the uncertainty relations. However, we will first examine the uncertainty relations for a point particle.

In the frame of a point particle, using the internal coordinates  $(x', y', z')$ , the wavefunction of the particle is given by a delta function at the origin:  $\delta(x')\delta(y')\delta(z')$ . This is given by the definition of a point particle. However, a delta-function wavefunction is not normalizable, which is a necessary condition for the proof of the uncertainty principle. We conclude that, instead, in the internal frame of a point particle, the position and momentum commute, and that there is no position-momentum uncertainty:

$$[x', \hat{p}_{x'}] = [y', \hat{p}_{y'}] = [z', \hat{p}_{z'}] = 0 \quad (1a)$$

$$\Delta x' \Delta p_{x'} = \Delta y' \Delta p_{y'} = \Delta z' \Delta p_{z'} = 0 \quad (1b)$$

In the frame of a point particle, both the position and momentum are zero:  $x' = y' = z' = 0$ , and  $p_{x'} = p_{y'} = p_{z'} = 0$ . Therefore, the position and momentum uncertainties are given by  $\Delta x' = \Delta y' = \Delta z' = 0$  and  $\Delta p_{x'} = \Delta p_{y'} = \Delta p_{z'} = 0$ , which are in agreement with Eq. (1). This particular application of Eq. (1) seems trivial and unuseful. However, the derivation of the angular uncertainty relations depend on the position and momentum commutation. Therefore, we determine that the angular momentum operators commute:

$$[\hat{J}_{x'}, \hat{J}_{y'}] = [\hat{J}_{x'}, \hat{J}_{z'}] = [\hat{J}_{y'}, \hat{J}_{z'}] = 0 \quad (2)$$

An important consequence of the commutation relations of Eq. (2) is that there are no raising and lowering operators in the internal coordinates, which implies that internal axis rotation by angle  $\theta$  is not possible. This makes sense physically, as the internal coordinates  $(x', y', z')$  are defined to be fixed with respect to the angular momentum  $\mathbf{j}$ . The internal consistency of the angular-momentum algebra is confirmed by the derivation of this fact, from the rotation matrices of the internal coordinates, given in Section V.3.

As  $n = |\mathbf{j}| = \sqrt{j(j+1)}$  is outside the range of  $-j$  to  $+j$ , it follows that the angular-momentum wavefunction  $D_{\sqrt{j(j+1)}, m}^j(\varphi, \theta, \chi)$  will be apparently unnormalizable. However, using an extension of a regularization procedure first introduced by Pandres [9], we show that the wavefunctions can be effectively normalized and that expectation values of operators can be calculated (we use the term regularization, and avoid the term “renormalization”, as this has a related but clearly different meaning in quantum electrodynamics). Despite these strange new properties, we make the case here that the  $D_{\sqrt{j(j+1)}, m}^j(\varphi, \theta, \chi)$  can be viewed as a useful spatial wavefunction of the angular momentum  $\mathbf{j}$  in the  $|jm\rangle$  state, and that significant geometrical information can be obtained from the  $D_{\sqrt{j(j+1)}, m}^j(\varphi, \theta, \chi)$  by calculating expectation values.

The internal projection  $n = \sqrt{l(l+1)}$  is sufficient for the description of orbital angular momentum  $\mathbf{l}$ , however we find that elementary particles with spin  $\mathbf{S}$  require at least the projections  $n = \sqrt{S(S+1)}$  and  $n = 0$ , to describe all the Standard Model particles. In this case,  $z'$  defines the axis of cylindrical

symmetry of the particle, and  $n$  is an intrinsic quantity of each fundamental particle, such the rest mass, charge, and spin  $S$ , and is invariant for each particle.

We note that recently we have shown that the asymptotic spatial wavefunction  $D_{(j+\frac{1}{2})m}^j(\varphi, \theta, \chi)$ , which treats the angular momentum  $\mathbf{j}$  as a three dimensional entity [10], is an excellent approximation for quantum-mechanical angular momentum:

$$D_{(j+\frac{1}{2})m}^j(\varphi, \theta, \chi) = e^{im\varphi} \delta(\theta - \theta_m) e^{i(j+\frac{1}{2})\chi} \quad (3)$$

where  $\theta_m$  is the Vector-Model polar angle, given by  $\cos\theta_m = m/|\mathbf{j}|$ . Note that in the high- $j$  limit, asymptotic magnitude of  $\mathbf{j}$  tends to  $j + \frac{1}{2}$  (as  $|\mathbf{j}| = \sqrt{j(j+1)} \rightarrow j + \frac{1}{2}$ ) so that  $D_{(j+\frac{1}{2})m}^j(\varphi, \theta, \chi)$  is the asymptotic limit of  $D_{\sqrt{j(j+1)},m}^j(\varphi, \theta, \chi)$ . The spatial wavefunction of Eq. (1) allows the geometrical description of Clebsch-Gordan coefficients, Wigner rotation matrix elements  $d_{m'm}^j(\varphi, \theta, \chi)$ , m-state correlation matrix elements, and the calculation of the gyromagnetic ratio of elementary charged particles at the tree level ( $g = 2$ ). These results are exact in the high- $j$  limit, but, surprisingly, they are either exact or an excellent approximation down to  $j = \frac{1}{2}$ . Clearly, it seems that an asymptotic spatial wavefunction for  $\mathbf{j}$  is a useful concept [10]. Based on the success of the unnormalizable wavefunction of Eq. (3), we ask whether the concept of an *exact* spatial wavefunction for  $\mathbf{j}$  extends to finite values of  $j$ .

To demonstrate the usefulness of the spatial-wavefunction formalism, we use the  $D_{n,m}^j(\varphi, \theta, \chi)$  to compute directly the gyromagnetic ratio of elementary charged particles with spin, by calculating the expectation value of the magnetic-moment operator. Interestingly,  $g = 2$  is computed for all values of spin, for  $S > 0$ . This agrees with the Dirac equation and Standard Model predictions for spins of  $\frac{1}{2}$  and 1, and confirms various arguments that  $g = 2$  is the natural tree-level gyromagnetic ratio for all values of spin [11,12].

In Section II, we describe the wavefunctions  $D_{n,m}^j(\varphi, \theta, \chi)$  as solutions of the space-fixed angular momentum operators  $\hat{\mathbf{J}}^2$ ,  $\hat{J}_Z$ , and  $\hat{J}_\pm$ . In Section III, we introduce the definition of

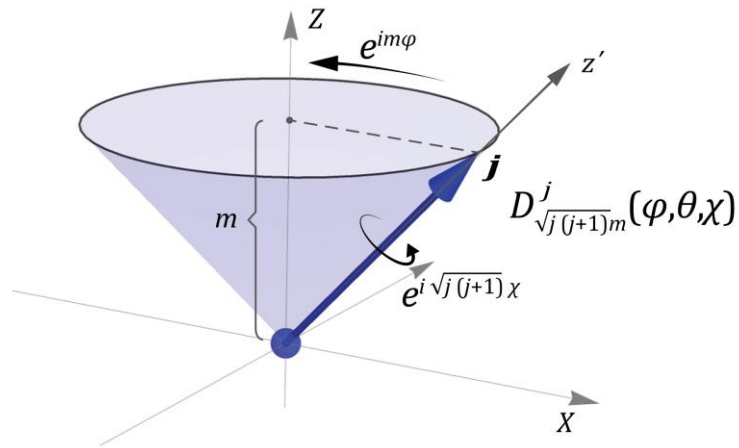


**Figure 3:** Depiction of the angular-momentum frame, where  $z'$  is defined as being parallel to  $\mathbf{j}$ . In this frame, the spin-wavefunction is given by  $D_{\sqrt{j(j+1)},m}^j(\varphi, \theta, \chi)$ , for which the angular momentum  $\mathbf{j}$  projects  $m$  along the space-fixed  $Z$  axis and  $|\mathbf{j}| = \sqrt{j(j+1)}$  along  $z'$ .

the inner product that allows the regularization of the  $D_{n,m}^j(\varphi, \theta, \chi)$ , and the calculation of the triple product of the  $D_{n,m}^j(\varphi, \theta, \chi)$  functions, needed for the calculation of expectation values. In Section IV we discuss the spatial distributions of the  $D_{\sqrt{j(j+1)},m}^j(\varphi, \theta, \chi)$  states, and how these connect with classical mechanics in the high- $j$  limit. In Section V we describe how the  $D_{n,m}^j(\varphi, \theta, \chi)$  are consistent with the usual angular momentum coupling and rotational transformations of the  $|jm\rangle$  states. In Section VI we calculate the  $g$  factor of spins of any  $S$ , from the expectation value of the magnetic moment operator. In Section VII we discuss how the spin wavefunctions of Standard Model particles  $D_{n,m}^S(\varphi, \theta, \chi)$  fall into two categories: those with  $n = \sqrt{S(S+1)}$  and those with  $n = 0$ ; we also present selection rules and a new conservation law, related to  $n$ , for particle reactions, from which we determine that the neutrino is a Dirac Fermion. In Section VIII we discuss how the new degree of freedom of the internal projection  $n$  (and  $n = 0$  in particular) opens the way for new dark-matter candidates, and we discuss one such possibility. In Section IX discuss some implications of the internal spin projections for the strong and the weak forces. Finally, in Section X we discuss the conclusions of our results.

## II. WAVEFUNCTIONS

We propose the spatial wavefunction of the angular momentum  $\mathbf{j}$  to be the  $D_{\sqrt{j(j+1)},m}^j(\varphi, \theta, \chi)$  Wigner D-functions, which connect asymptotically to those of Eq. (1), to be:

$$D_{\sqrt{j(j+1)},m}^j(\varphi, \theta, \chi) = e^{im\varphi} d_{\sqrt{j(j+1)},m}^j(\theta) e^{i\sqrt{j(j+1)}\chi} \quad (4)$$

However, we will investigate the more general solution,  $D_{n,m}^j(\varphi, \theta, \chi)$ , for which the projection  $n$  along  $z'$  can take any value:

$$D_{n,m}^j(\varphi, \theta, \chi) = e^{im\varphi} d_{n,m}^j(\theta) e^{in\chi} \quad (5)$$

where  $m$  is the projection of the angular momentum  $\mathbf{j}$  along the  $Z$  axis. The requirement that  $D_{n,m}^j(\varphi, \theta, \chi)$  be directly normalizable constrains  $m$  and  $n$  to range from  $-j$  to  $+j$ , in integer steps, as is the case for the well-known Wigner D-functions  $D_{m',m}^j(\varphi, \theta, \chi)$ . For the  $D_{n,m}^j(\varphi, \theta, \chi)$  we use the more general body-fixed projection  $n$ , because in this Section we will treat  $n$  as a continuous variable, for values outside of the normal range of  $-j$  to  $+j$ , to better understand the properties of the  $D_{n,m}^j(\varphi, \theta, \chi)$ .

The  $D_{n,m}^j(\varphi, \theta, \chi)$  wavefunctions are clearly eigenfunctions of the space-fixed angular momentum operator  $\hat{J}_Z$ , given by (using  $\hbar = 1$ ) [13]:

$$\hat{J}_Z = -i \frac{\partial}{\partial \varphi} \quad (6)$$

yielding eigenvalue  $m$ , corresponding to the projection of  $\mathbf{j}$  along the  $Z$ .

The  $D_{nm}^j(\varphi, \theta, \chi)$  wavefunctions are also eigenfunctions of the body-fixed angular momentum operator  $\hat{J}_{z'}$ , given by (using  $\hbar = 1$ ) [14]:

$$\hat{J}_{z'} = -i \frac{\partial}{\partial \chi} \quad (7)$$

yielding eigenvalue  $n = n_{z'} = \sqrt{j(j+1)}$ , corresponding to the full projection of  $\mathbf{j}$  along the  $z'$ , so that the perpendicular projections are zero:

$n_{x'} = n_{y'} = 0$ . By symmetry, we have

two more orthogonal solutions, with

the spin fully parallel to the  $x'$  or  $y'$

axes, with :  $n_{x'} = \sqrt{j(j+1)}$ ,  $n_{y'} =$

$n_{z'} = 0$ , and  $n_{y'} = \sqrt{j(j+1)}$ ,  $n_{x'} =$

$n_{z'} = 0$  (see Fig. 4). These three states

span the internal-coordinate spin-

space, and any other states can be

expressed as linear combinations of

these three orthogonal states. The

$n_{x'} = \sqrt{j(j+1)}$  and  $n_{y'} = \sqrt{j(j+1)}$

states can be described as doubly degenerate  $n = n_{z'} = 0$  state.

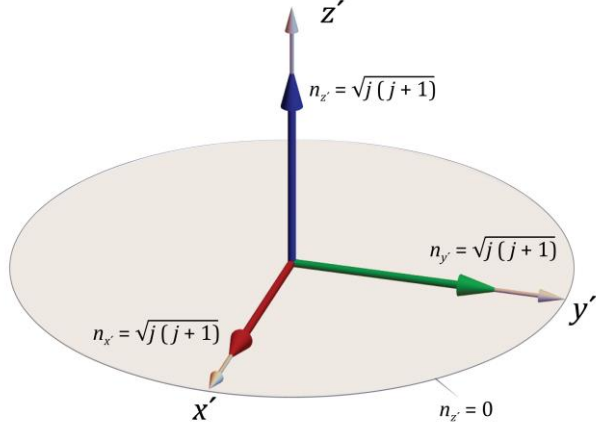


*Figure 4: Depiction of the three orthogonal internal-coordinate spin-projection states, along the  $z'$  axis with  $n_{z'} = \sqrt{j(j+1)}$ , the  $x'$  axis with  $n_{x'} = \sqrt{j(j+1)}$ , and the  $y'$  axis with  $n_{y'} = \sqrt{j(j+1)}$ ; the latter two can be described by a doubly degenerate  $n_{z'} = 0$  state.*

The  $D_{nm}^j(\varphi, \theta, \chi)$  must also be eigenfunctions of the  $\hat{J}^2$  operator, given by [13]:

$$\hat{J}^2 = -\left\{ \frac{\partial^2}{\partial \theta^2} + \cot \theta \frac{\partial}{\partial \theta} + \frac{1}{\sin^2 \theta} \left( \frac{\partial^2}{\partial \varphi^2} + \frac{\partial^2}{\partial \chi^2} - 2 \cos \theta \frac{\partial^2}{\partial \varphi \partial \chi} \right) \right\} \quad (8)$$

Operating  $\hat{J}^2$  on  $D_{nm}^j(\varphi, \theta, \chi)$  in Eq. (4) yields the eigenvalue  $j(j+1)$ , and evaluating the derivatives

in  $\varphi$  and  $\chi$  gives a differential equation in  $\theta$  for  $d_{nm}^j(\theta)$ :

$$\left[ \frac{\partial^2}{\partial \theta^2} + \cot \theta \frac{\partial}{\partial \theta} - \frac{1}{\sin^2 \theta} (m^2 + n^2 - 2mn \cos \theta) + j(j+1) \right] d_{nm}^j(\theta) = 0 \quad (9)$$

The general solution for  $d_{nm}^j(\theta)$  is given by:

$$d_{nm}^j(\theta) = \left[ A \left( \sin \frac{\theta}{2} \right)^{m-n} \left( \cos \frac{\theta}{2} \right)^{m+n} {}_2F_1 \left( m-j, m+j+1; 1+m-n; \sin^2 \frac{\theta}{2} \right) + B \left( \sin \frac{\theta}{2} \right)^{n-m} \left( \cos \frac{\theta}{2} \right)^{n+m} {}_2F_1 \left( n-j, n+j+1; 1+n-m; \sin^2 \frac{\theta}{2} \right) \right] \quad (10)$$

where  ${}_2F_1(a, b; c; z)$  is the Gaussian hypergeometric function, and  $A$  and  $B$  are constants. Note that for

$n = m'$  (where  $m'$  ranges from  $-j$  to  $j$  in integer steps), Eq. (10) reduces to the conventional Wigner

$d_{m' m}^j(\theta)$  functions.

The operator  $\hat{J}_{\pm}$  raises or lowers the  $m$  quantum number:

$$\hat{J}_{\pm} D_{n,m}^j(\varphi, \theta, \chi) = \sqrt{j(j+1) - m(m \pm 1)} D_{n, m \pm 1}^j(\varphi, \theta, \chi) \quad (11)$$

and is given by [13]:

$$\hat{J}_{\pm} = e^{\pm i\varphi} \left\{ i \left[ \cot \theta \frac{\partial}{\partial \varphi} - \frac{1}{\sin \theta} \frac{\partial}{\partial \chi} \right] \pm \frac{\partial}{\partial \theta} \right\} \quad (12)$$

An apparent exception to the standard rule of Eq. (11) are the maximum projection states, where a non-zero function seems to be given, with projection  $m = \pm(j+1)$ , beyond the physical range:

$$\hat{J}_{\pm} D_{n, \pm j}^j(\varphi, \theta, \chi) = D_{n, \pm(j+1)}^j(\varphi, \theta, \chi) \quad (13)$$

However, using work by Pandres and others [9,15,16], it can be demonstrated that the states  $D_{n, \pm(j+1)}^j(\varphi, \theta, \chi)$  are vanishing functions, as shown by two facts: (1) lowering/raising them back to  $m = \pm j$  yields zero (see Appendix A):

$$\hat{J}_{\mp} D_{n, \pm(j+1)}^j(\varphi, \theta, \chi) = 0 \quad (14)$$

and (2) their norms (defined in Section III) also vanish:

$$\left\langle D_{n, \pm(j+1)}^j(\varphi, \theta, \chi) \mid D_{n, \pm(j+1)}^j(\varphi, \theta, \chi) \right\rangle = 0 \quad (15)$$

Using the general solution of Eq. (10), we give expressions for the  $d_{n,m}^j(\theta)$  for spin 0 (which is simply a constant):

$$d_{n,0}^0(\theta) = N_0 \quad (16)$$

for spin  $\frac{1}{2}$ :

$$d_{n,1/2}^{\frac{1}{2}}(\theta) = N_{1/2} \left[ e^{\frac{i\pi}{4}} \left( \cos \frac{\theta}{2} \right)^{\frac{1}{2}+n} \left( \sin \frac{\theta}{2} \right)^{\frac{1}{2}-n} + e^{-\frac{i\pi}{4}} \left( \cos \frac{\theta}{2} \right)^{\frac{1}{2}-n} \left( \sin \frac{\theta}{2} \right)^{n-\frac{1}{2}} \left( n + \frac{1}{2} \cos \theta \right) \right] \quad (17a)$$

$$d_{n,-1/2}^{\frac{1}{2}}(\theta) = N_{1/2} \left[ e^{\frac{i\pi}{4}} \left( \cos \frac{\theta}{2} \right)^{n-\frac{1}{2}} \left( \sin \frac{\theta}{2} \right)^{\frac{1}{2}-n} \left( n - \frac{1}{2} \cos \theta \right) + e^{-\frac{i\pi}{4}} \left( \cos \frac{\theta}{2} \right)^{\frac{1}{2}-n} \left( \sin \frac{\theta}{2} \right)^{\frac{1}{2}+n} \right] \quad (17b)$$

and for spin 1:

$$d_{n,1}^1(\theta) = N_1 \left[ e^{\frac{i\pi}{4}} \left( \cos \frac{\theta}{2} \right)^{1+n} \left( \sin \frac{\theta}{2} \right)^{1-n} + \frac{e^{-\frac{i\pi}{4}} \left( \cos \frac{\theta}{2} \right)^{-n-1} \left( \sin \frac{\theta}{2} \right)^{n-1} \left( n^2 + n \cos \theta - \frac{1}{2} \sin^2 \theta \right)}{2} \right] \quad (18a)$$

$$d_{n,0}^1(\theta) = N_1 \left[ \frac{e^{\frac{i\pi}{4}} \left( \cos \frac{\theta}{2} \right)^n \left( \sin \frac{\theta}{2} \right)^{-n} \left( n - \cos \theta \right) + e^{-\frac{i\pi}{4}} \left( \cos \frac{\theta}{2} \right)^{-n} \left( \sin \frac{\theta}{2} \right)^n \left( n + \cos \theta \right)}{\sqrt{2}} \right] \quad (18b)$$

$$d_{n,-1}^1(\theta) = N_1 \left[ \frac{e^{\frac{i\pi}{4}} \left( \cos \frac{\theta}{2} \right)^{n-1} \left( \sin \frac{\theta}{2} \right)^{-n-1} \left( n^2 - n \cos \theta - \frac{1}{2} \sin^2 \theta \right)}{2} + e^{-\frac{i\pi}{4}} \left( \cos \frac{\theta}{2} \right)^{1-n} \left( \sin \frac{\theta}{2} \right)^{1+n} \right] \quad (18c)$$

where the  $N_j$  are normalization constants, and the constants  $A$  and  $B$  in Eq. (10) have been chosen so that the  $(2j+1)$ -degenerate group of  $D_{n,m}^j(\varphi, \theta, \chi)$  satisfy Eqs. (11-14) and are geometrically symmetric: lowering/raising from  $\pm m$  to  $\mp m$  corresponds to the geometrical transformation  $\theta \rightarrow \pi -$

$\theta$ , along with complex conjugation, which gives  $\cos \frac{\theta}{2} \rightarrow \sin \frac{\theta}{2}$ ,  $\sin \frac{\theta}{2} \rightarrow \cos \frac{\theta}{2}$ ,  $\cos \theta \rightarrow -\cos \theta$ , and sign reversal of the phase factors  $e^{\pm im\varphi} \rightarrow e^{\mp im\varphi}$  and  $e^{\pm \frac{i\pi}{4}} \rightarrow e^{\mp \frac{i\pi}{4}}$ . Notice that for this geometrical transformation,  $D_{n,\pm m}^j(\varphi, \theta, \chi) \rightarrow D_{n,\mp m}^j(\varphi, \theta, \chi)$ . In addition, notice that for the geometrical transformations  $\theta \rightarrow \theta + 2\pi$  or  $\varphi \rightarrow \varphi + 2\pi$ , that  $D_{n,m}^j(\varphi, \theta, \chi) \rightarrow (-1)^{2j} D_{n,m}^j(\varphi, \theta, \chi)$ , so that functions with half-integer  $j$  change sign, whereas those with integer  $j$  do not.

Wavefunctions for any  $j$  can be generated by setting the first term of the  $d_{n,j}^j$  state as  $e^{\frac{i\pi}{4}} \left(\cos \frac{\theta}{2}\right)^{j+n} \left(\sin \frac{\theta}{2}\right)^{j-n}$ ; subsequently all the first terms of the states down to  $m = -j$  are produced by operating  $\hat{J}_-$  sequentially on  $D_{n,j}^j$ . Similarly, the second term of the  $d_{n,-j}^j$  state is set as  $e^{-\frac{i\pi}{4}} \left(\sin \frac{\theta}{2}\right)^{j+n} \left(\cos \frac{\theta}{2}\right)^{j-n}$ , and the second terms of the states up to  $m = +j$  are produced by operating  $\hat{J}_+$  sequentially on  $D_{n,-j}^j$ . In both cases, after each operation of  $\hat{J}_{\pm}$ , the result must be divided by the factor  $\sqrt{j(j+1) - m(m \pm 1)}$ , from Eq. (11).

### III. INNER PRODUCT REGULARIZATION AND EXPECTATION VALUES

The expressions of Eqs. (17-18) are unnormalizable for  $n = \sqrt{j(j+1)}$ , because at least one term in each expression gives a divergent integral. In fact, in general, all terms for all values of  $j$  are divergent, except for one term of the maximum projection states. To renormalize these expressions, we use an extension of the definition of the inner product  $\langle \Psi | \Psi' \rangle$  given by Pandres [9] for half-integer spherical harmonics (to include an integral over the angle  $\chi$ , over an infinite domain):

$$\langle \Psi | \Psi' \rangle = \int_0^{\pi} d\theta \left[ \sin \theta \int_0^{2\pi} d\varphi \int_0^{2\pi q} \lim_{q \rightarrow \infty} \frac{1}{2\pi q} d\chi \Psi^*(\varphi, \theta, \chi) \Psi'(\varphi, \theta, \chi) - f(\theta) \right] \quad (19a)$$

where  $f(\theta)$  is:

$$f(\theta) = \sum_{m=1}^{\infty} a_m (\sin \theta)^{-m} + \cos \theta \sum_{m=1}^{\infty} b_m (\sin \theta)^{-m}, \quad (19b)$$

and the constants  $a_m$  and  $b_m$  are chosen so that diverging terms in  $\Psi^* \Psi' \sin \theta$ , which are proportional to negative powers of  $\sin \theta$ , are cancelled. Note that  $\Psi^* \Psi' \sin \theta$  is first expanded in powers of  $\sin \theta$ , to separate terms with negative powers (that diverge) from non-negative powers (that don't diverge).

Equation (16) allows the renormalization of the  $D_{n,m}^j(\varphi, \theta, \chi)$  for  $n = \sqrt{j(j+1)}$ . The actual value of the normalization constant  $N_j$  is not relevant for two reasons: (1) the unnormalizable state cannot be used to calculate the direct angular distribution of  $\mathbf{j}$ , as only expectation values can be calculated, and (2) expectation values are expressed as a ratio where  $N_j$  cancels.

The inner product can be used to show analytically that:

$$\left\langle D_{n',m'}^j(\varphi, \theta, \chi) \mid D_{n,m}^j(\varphi, \theta, \chi) \right\rangle = \delta_{n'n} \delta_{m'm} \quad \text{for } -j \leq n \leq +j \quad (20)$$

without renormalization, as these wavefunctions are normalizable. For  $|n| > j$  Eq. (19) will renormalize the inner product for all  $n$ .

The integral of the triple product of  $D_{m',m}^j(R)$  functions is given by [13]:

$$\left\langle D_{m'_1 m_1}^{j_1}(R) \mid D_{m'_2 m_2}^{j_2}(R) \mid D_{m'_3 m_3}^{j_3}(R) \right\rangle = \frac{8\pi^2}{2j_3+1} \langle j_1 m_1, j_2 m_2 \mid j_3 m_3 \rangle \langle j_1 m'_1, j_2 m'_2 \mid j_3 m'_3 \rangle \quad (21a)$$

Importantly, Eq. (16) allows the extension of the integral of Eq. (21a), of the triple product of  $D_{m',m}^j(R)$  functions, to those of  $D_{nm}^j(R)$  functions, for any value of  $n$ , for which two of the D-functions have same value of  $j$  and  $n$ , and for the third has  $n = 0$ :

$$\left\langle D_{nm}^j(R) \mid D_{0q}^k(R) \mid D_{nm'}^j(R) \right\rangle = \langle j n, k 0 \mid j n \rangle \langle j m, k q \mid j m' \rangle \quad (21b)$$

Note that: Eq. (18b) allows the calculation of expectation values of  $D_{nm}^j(R)$  wavefunctions for any  $n$ ; the  $D_{0q}^k(R)$  are proportional to the spherical harmonics  $Y_q^k(\theta, \varphi)$ , which span the space of all angular functions, so that the expectation value of the angular part of any operator can be calculated; the factor of  $8\pi^2/(2j_3 + 1)$  in Eq. (18a) is absent in Eq. (21b), because the  $D_{nm}^j(R)$  are normalized (whereas the  $D_{m',m}^j(R)$  are not). The validity of Eq. (21b) for any value of  $n$  in the range  $-j \leq n \leq +j$  can be easily verified analytically. In Appendix B, we demonstrate a calculation for the expectation value of  $\cos\theta$  for  $j = m = 1/2$ , and  $n = 1$ ; as  $n > \sqrt{j(j+1)}$ , we must use the regularization of Eq. 19.

Note also that the ClebschGordan coefficients of the form  $\langle j n, k 0 \mid j n \rangle$  have analytical expressions, which are mathematically valid for any value of  $n$ ; for example, we give the values for  $k$  ranging from 1 to 4:

$$\langle j n, 1 0 \mid j n \rangle = \frac{n}{\sqrt{j(j+1)}} = P_1(\cos\theta_n) \quad (22a)$$

$$\langle j n, 2 0 \mid j n \rangle = \sqrt{\frac{j(j+1)}{(j+1/2)(j+3/2)}} P_2(\cos\theta_n) \quad (22b)$$

$$\langle j n, 3 0 \mid j n \rangle = \frac{j(j+1)}{\sqrt{(j-1)(j-1/2)(j+3/2)(j+2)}} \left[ P_3(\cos\theta_n) + \frac{\cos\theta_n}{2j(j+1)} \right] \quad (22c)$$

$$\langle j n, 4 0 \mid j n \rangle = \sqrt{\frac{j^3(j+1)^3}{(j-3/2)(j-1)(j-1/2)(j+3/2)(j+2)(j+5/2)}} \left[ P_4(\cos\theta_n) + \frac{25 \cos^2 \theta_n - 6}{8j(j+1)} \right] \quad (22d)$$

where  $\cos\theta_n = n/\sqrt{j(j+1)}$ . The physical requirement that the probability amplitude ranges from  $-1$  to  $+1$  constrains the value of  $n$  to be in the range of  $-\sqrt{j(j+1)}$  to  $+\sqrt{j(j+1)}$ , for  $\langle j n, 1 0 \mid j n \rangle$  (other Clebsch-Gordan coefficients will have other constraints, depending on the value of  $k$  and  $j$ ). In the next section, we use Eq. (19) to examine the angular distribution of orbital angular momentum.

#### IV. ANGULAR MOMENTUM SPATIAL DISTRIBUTIONS

The spatial distribution of a spatial wavefunction is given by the square  $\left|D_{\sqrt{j(j+1)}m}^j(\varphi, \theta, \chi)\right|^2$ .

However, with the exception of the trivial case of the  $j = 0$  state (where  $\left|D_{0,0}^0(\varphi, \theta, \chi)\right|^2 = N_0^2$  is constant with no dependence on angles), these squares are unnormalizable, so that the angular distribution of  $\mathbf{j}$  does not correspond to an observable.

However, the magnetic moment  $\boldsymbol{\mu}$  of  $\mathbf{j}$  can be probed with a magnetic field  $\mathbf{B}$ , through the interaction Hamiltonian  $H = -\boldsymbol{\mu} \cdot \mathbf{B} = |\boldsymbol{\mu}||\mathbf{B}|\cos\theta$ . The expectation value of  $\cos\theta$  can be calculated using Eq. (21b):

$$\left\langle D_{\sqrt{j(j+1)}m}^j(R) \left| D_{0,0}^1(R) \right| D_{\sqrt{j(j+1)}m}^j(R) \right\rangle = \langle j \sqrt{j(j+1)}, 1 \ 0 | j \sqrt{j(j+1)} \rangle \langle j \ m, k \ 0 | j \ m \rangle \quad (23)$$

where  $\cos\theta = D_{0,0}^1(0, \theta, 0)$ , and  $\langle j \sqrt{j(j+1)}, 1 \ 0 | j \sqrt{j(j+1)} \rangle = 1$ , from Eq. (22a), and thus:

$$\langle \cos\theta \rangle = \frac{m}{\sqrt{l(l+1)}} = \cos\theta_m \quad (24)$$

Which agrees with known quantum mechanics and the Vector Model.

We then investigate the limit  $l \rightarrow \infty$ , and the calculation of  $\langle P_k(\cos\theta) \rangle$  for all  $k$ .

The Clebsch-Gordan coefficient  $\langle l \sqrt{l(l+1)}, k \ 0 | l \sqrt{l(l+1)} \rangle$  can be written in the form:

$$\langle l \sqrt{l(l+1)}, k \ 0 | l \sqrt{l(l+1)} \rangle = U_k(l) \left[ P_k(\cos\theta) + \frac{f(\theta)}{l(l+1)} \right] \quad (25)$$

where  $U_k(l)$  is a constant, and  $f(\theta)$  is proportional to powers of  $\cos\theta$  up to rank  $(k - 2)$ . In the limit of  $l \rightarrow \infty$ ,  $U_k(l) \rightarrow 1$  and  $f(\theta)/l(l+1) \rightarrow 0$ , so that  $\langle l \sqrt{l(l+1)}, k \ 0 | l \sqrt{l(l+1)} \rangle \rightarrow 1$ , and the expectation values  $\langle P_k(\cos\theta) \rangle$  become well defined. Specifically, in this limit,  $\langle j \ m, k \ 0 | j \ m \rangle \rightarrow P_k(\cos\theta_m)$ , so that:

$$\langle P_k(\cos\theta) \rangle \rightarrow P_k(\cos\theta_m) \quad \text{as } l \rightarrow \infty \quad (26)$$

where  $\cos\theta_m = m/\sqrt{l(l+1)}$ . This limit of the expectation value of Eq. (26) is consistent with the classical limit of the Vector Model:

$$\left| D_{\sqrt{l(l+1)}m}^l(\varphi, \theta, \chi) \right|^2 \rightarrow \delta(\theta - \theta_m) \quad \text{as } l \rightarrow \infty \quad (27)$$

We conclude that the expectation values  $\langle P_k(\cos\theta) \rangle$  agree with known quantum mechanics: for  $k = 1$   $\langle \cos\theta \rangle$  gives the well-known projection of  $\mathbf{l}$  along the Z axis, in Eq. (24). In the classical limit of  $l \rightarrow \infty$ , the  $\langle P_k(\cos\theta) \rangle$  and  $\left| D_{\sqrt{l(l+1)}m}^l(\varphi, \theta, \chi) \right|^2$  give values consistent with the classical limit of the Vector Model, given by Eqs. (23) and (24), and the full spatial distribution of  $\mathbf{l}$  becomes consistent with the

semiclassical limit (see also the discussion of angular momentum wavepackets in [10]).

## V. CLEBSCH-GORDAN COEFFICIENTS AND WIGNER D-FUNCTIONS

1. *Clebsch-Gordan coefficients.* For the inner product in Eq. (19),  $\hat{J}_+$  and  $\hat{J}_-$  are mutual Hermitian adjoints (proved similarly as in the Appendix of [9]):

$$\langle \hat{J}_+ \Psi | \Psi' \rangle = \langle \Psi | \hat{J}_- \Psi' \rangle \quad (28)$$

Using Eq. (25), it is straightforward to show that [9]:

$$\left\langle D_{nm}^j(\varphi, \theta, \chi) \mid D_{n'm'}^{j'}(\varphi, \theta, \chi) \right\rangle = \delta_{jj'} \delta_{nn'} \delta_{mm'} \quad (\text{for } |m|, |m'| \leq j) \quad (29a)$$

$$\left\langle D_{nm}^j(\varphi, \theta, \chi) \mid D_{n'm'}^{j'}(\varphi, \theta, \chi) \right\rangle = 0 \quad (\text{for } |m| \text{ or } |m'| > j) \quad (29b)$$

As the  $D_{nm}^j$  functions form an orthonormal set [examples given in Eqs. (17-18)] and obey Eq. (8), all Clebsch-Gordan coefficients can be calculated in the usual way using the lowering operator  $\hat{J}_-$  [13,17].

2. *Wigner D-functions for space-fixed-axes rotations.* The usual Wigner rotation matrix elements  $d_{m_1' m_1}^{j_1}(\theta)$  [13,17,18], for rotations in the space-fixed axis, can be expressed in terms of a Clebsch-Gordan coefficient, where the  $|j_1 m_1\rangle$  state is coupled to an infinite angular momentum  $j_2$  at angle  $\theta$  to the Z axis [10]:

$$d_{m_1' m_1}^{j_1}(\theta) = (-1)^{j_1 - m_1'} \lim_{j_2 \rightarrow \infty} \langle j_1 m_1, j_2 m_2 \mid j_2 + m_1', m_1 + m_2 \rangle \quad (30)$$

where  $\cos \theta = m_2 / j_2$ ; note that  $m_2 = j_2 \cos \theta$  also tends to infinity. This coupled state decouples uniquely to the  $|j_1 m_1'\rangle$  state along the  $z'$  quantization axis (parallel to  $j_2$ ):

$$\lim_{j_2 \rightarrow \infty} \langle j_2 + m_1', j_2 + m_1' \mid j_2 j_2, j_1 m_1' \rangle = 1 \quad (31)$$

Therefore, Eqs. (23-24) describe the probability amplitude that the  $|j_1 m_1\rangle$  state, along Z, is projected to the  $|j_1 m_1'\rangle$  state along a new quantization axis  $z'$ , at angle  $\theta$  to Z, which is the definition of  $d_{m_1' m_1}^{j_1}(\theta)$ .

Therefore, Eq. (23) shows that the  $D_{nm}^j$  functions transform under rotation as the  $|jm\rangle$  state.

We demonstrate this for  $S=1/2$ , using the general Clebsch-Gordan coefficient for the  $\left|\frac{1}{2} \frac{1}{2}\right\rangle$  state [13]:

$$\left\langle \frac{1}{2} \frac{1}{2}, j_2 m_2 \mid j_2 \pm \frac{1}{2}, m_2 + \frac{1}{2} \right\rangle = \sqrt{\frac{j_2 \pm m_2 + 1}{2j_2 + 1}} \quad (32)$$

Inserting Eq. (29) into Eq. (27) yields, for  $m_1' = \frac{1}{2}$  and  $-\frac{1}{2}$ , and using  $m_2 = j_2 \cos \theta$ :

$$d_{\frac{1}{2} \frac{1}{2}}^{\frac{1}{2}}(\theta) = d_{-\frac{1}{2} \frac{1}{2}}^{\frac{1}{2}}(\theta) = \lim_{j_2 \rightarrow \infty} \sqrt{\frac{j_2(1+\cos \theta)+1}{2j_2+1}} = \sqrt{\frac{(1+\cos \theta)}{2}} = \cos \frac{\theta}{2} \quad (33a)$$

$$d_{\frac{1}{2} -\frac{1}{2}}^{\frac{1}{2}}(\theta) = -d_{-\frac{1}{2} -\frac{1}{2}}^{\frac{1}{2}}(\theta) = \lim_{j_2 \rightarrow \infty} \sqrt{\frac{j_2(1-\cos \theta)+1}{2j_2+1}} = \sqrt{\frac{(1-\cos \theta)}{2}} = \sin \frac{\theta}{2} \quad (33b)$$

showing, as expected, that the  $D_{nm}^{\frac{1}{2}}(\varphi, \theta, \chi)$  transform under rotation as spinors.

3. *Wigner D-functions for body-fixed-axes rotations.* We defined the body-fixed  $z'$  axis to be exactly parallel to the angular momentum  $\mathbf{j}$  (or parallel to the internal body-fixed symmetry axis of an elementary particle). This definition seems to preclude any body-fixed-axis rotation of the  $z'$  axis, as it is fixed with respect to  $\mathbf{j}$  (or the body-fixed axis), by definition. We examine the internal consistency of the angular momentum algebra, by considering the Wigner rotation matrix  $d_{n,n}^j(\theta)$ , which gives the probability amplitude for the rotation of the  $z'$  axis by angle  $\theta$ . The  $d_{n,n}^j(\theta)$  function is unnormalizable for  $n = \sqrt{j(j+1)}$ , however, we can calculate the expectation value of  $\cos\theta$ , using Eq. (21b):

$$\langle \cos\theta \rangle = \left\langle d_{n,n}^j(\theta) |d_{0,0}^1(\theta) |d_{n,n}^j(\theta) \right\rangle = \langle j, n, 1, 0 | j, n \rangle^2 = \frac{n^2}{j(j+1)} \quad (34)$$

where  $\langle j, n, 1, 0 | j, n \rangle$  is given by Eq. (19a). For  $n = \sqrt{j(j+1)}$ , Eq. (31) gives that  $\langle \cos\theta \rangle = 1$ , which can be interpreted by the fact that the regularized  $|d_{n,n}^j(\theta)|^2$  distribution has all the probability distribution at  $\theta = 0$ , equivalent to  $\delta(\theta)$ , i.e., the  $D_{n,m}^j(\varphi, \theta, \chi)$  with  $n = \sqrt{j(j+1)}$  cannot be rotated to change the projection  $n$ . This argument applies to all three of the orthogonal states (shown in Fig. 4), as they each correspond to a maximum projection state:  $n_{z'} = \sqrt{j(j+1)}$ , or  $n_{x'} = \sqrt{j(j+1)}$ , or  $n_{y'} = \sqrt{j(j+1)}$ .

## VI. G-FACTOR CALCULATION

We now use the spin wavefunctions to calculate the g factor of an elementary particle, which has mass  $m$ , charge  $e$ , spin  $S$ , and a spatial angular momentum wavefunction  $\psi_{spin}(\varphi, \theta, \chi) = D_{n,m}^S(\varphi, \theta, \chi)$  (given by Eq. (4), with  $S=j$ ). It will have magnetic moment components  $\hat{\mu}_Z$  and  $\hat{\mu}_{z'}$ , along the  $Z$  and  $z'$  axes, respectively, given by:

$$\hat{\mu}_Z = \mu_B \hat{S}_Z = -i\mu_B \frac{\partial}{\partial \varphi} \quad (35a)$$

$$\hat{\mu}_{z'} = \mu_B \hat{S}_{z'} = -i\mu_B \frac{\partial}{\partial \chi} \quad (35b)$$

where the Bohr magneton  $\mu_B = e\hbar/2m$ . The  $z'$  axis is at angle  $\theta$  to  $Z$ , and distributed about  $Z$  with cylindrical symmetry, so that only the parallel component of  $\mu_{z'}$  contributes to the total magnetic moment along  $Z$ :

$$\hat{\mu}_Z^T = \hat{\mu}_Z + \cos\theta \hat{\mu}_{z'} \quad (36)$$

The magnetic moment is then given by the expectation value of  $\hat{\mu}_Z^T$  for the state  $D_{n,M}^S(\varphi, \theta, \chi)$ , given by:

$$\langle \hat{\mu}_Z^T \rangle = \langle D_{n,M}^S | \hat{\mu}_Z^T | D_{n,M}^S \rangle = \mu_B \left( M + n \langle D_{n,M}^S | \cos\theta | D_{n,M}^S \rangle \right) = \mu_B M \left( 1 + \frac{n^2}{S(S+1)} \right) \quad (37)$$

where the expectation value  $\langle \cos\theta \rangle = nM/S(S+1)$  is given by Eq. (18b). The magnetic moment of the maximum projection state of an elementary particle is expressed generally as  $gM\mu_B$ , so that we find

in general:

$$g = \left(1 + \frac{n^2}{S(S+1)}\right) \quad (38)$$

Requiring that  $g = 2$  (at the tree level) for charged particles independent of the value of  $S$  [19], gives a clear geometrical interpretation (and without relativistic considerations [17,20]): we see that the projection of  $\mathbf{S}$  along the body-fixed  $z'$  axis must be maximal,  $n = \sqrt{S(S+1)}$ , and a magnetic moment points along  $\mathbf{S}$  with magnitude  $\mu_B \sqrt{S(S+1)}$ , as shown in Fig. 3; also,  $\hat{\mu}_z$  and  $\hat{\mu}_{z'}$  contribute equally to the magnetic moment of the particle.

We note that this straightforward geometric calculation of  $g = 2$  for all  $S$  (given  $n = \sqrt{S(S+1)}$ ) cannot be calculated straightforwardly in standard quantum mechanics for  $S > 1$  [11,12]. The interaction of a charged particle with spin  $S = 1/2$  with an electromagnetic field can be performed by substituting the derivative of charged fields in the Lagrangian with the covariant derivative [21]:

$$\partial_\mu \varphi \rightarrow \partial_\mu \varphi + ieA_\mu \quad (39)$$

where  $e$  is the electric charge of the field  $\varphi$ , and the  $A_\mu$  are the components of the magnetic vector potential. The substitution of Eq. (39) is known as the “minimal substitution” or “minimal coupling”, and it correctly yields  $g = 2$  for  $S = 1/2$ . Using “minimal coupling” in the Proca equation for  $S = 1$  [22] yields  $g = 1$ . Belinfante then calculated  $g = 2/3$  for  $S = 3/2$ , and subsequently proposed the Belinfante conjecture [23]: that  $g = 1/S$ , for all spins  $S$ . However, the charged W boson with  $S = 1$  is observed to have  $g = 2$  [24], experimentally refuting Belinfante’s conjecture, and showing that “minimal coupling” is not sufficient; the requirement that the Lagrangian be gauge invariant adds an extra term to the Lagrangian [25], which then gives  $g = 2$ .

Several arguments are given elsewhere [11,12] that  $g = 2$  is the natural value for all elementary charged particles with any spin  $S$ . Here, we add an additional geometric argument: that  $g = 2$  for any spin  $S$  corresponds to  $\mathbf{S}$  and the magnetic moment  $\boldsymbol{\mu}$  being parallel or antiparallel to  $z'$  (the symmetry axis of the particle, with  $n = \sqrt{S(S+1)}$ , as shown in Fig. 3, where  $z'$  defines the body-fixed axis of the  $D_{nm}^S(\varphi, \theta, \chi)$  symmetric-top wavefunction). In contrast, solving Eq. (38) for the Belinfante conjecture of  $g = 1/S$  yields  $n = \sqrt{(1 - S^2)}$ . This result, although it gives the correct result for  $S = 1/2$  (that  $n = \sqrt{3}/2 = \sqrt{S(S+1)}$ ), gives the physically meaningless result that  $n$  is imaginary for  $S > 1$ .

## VII. IMPLICATIONS FOR STANDARD-MODEL PARTICLES: DIRAC FERMION NATURE OF NEUTRINO

From Section VI we see that all charged fundamental particles with spin  $S$  (i.e., the quarks, electrons, and the W boson) must have internal projection  $n = \sqrt{S(S+1)}$ . However, neutral particles that are their

own antiparticle must have all internal quantum numbers be 0, so that  $n = 0$  (e.g., for the photon and the Z boson, and also for the gluons).

We first consider the decay of an  $n = 0$  particle with spin  $S_i$  and  $M_i = S_i$ , into a pair of  $n = 0$  particles each with spin  $S_f$  and  $M_f = S_i/2$ . The probability of the decay will be proportional to the overlap integral of the spin wavefunctions:

$$\left\langle D_{0 S_i}^{S_i}(R) \middle| D_{0 S_i/2}^{S_f}(R) D_{0 S_i/2}^{S_f}(R) \right\rangle = \langle S_i 0 | S_f 0, S_f 0 \rangle \langle S_i S_i | S_f S_i/2, S_f S_i/2 \rangle \quad (40)$$

The fact that the decay probability is proportional to the simple Clebsch-Gordan coefficient  $\langle S_i 0 | S 0, S 0 \rangle$  allows us to draw some simple conclusions:  $\langle S_i 0 | S_f 0, S_f 0 \rangle = 0$  for odd values of  $S_i$ , therefore the decay of an  $n = 0$  particle with odd spin  $S_i$  *cannot* decay into two  $n = 0$  particles. This statement, and Eq. (40), is a generalization of the Landau-Yang theorem [26,27]. The Landau-Yang theorem has been used to justify why, for example, the Z boson cannot decay to 2 photons. By using Eq. (40), we extend predictions beyond the Landau-Yang theorem, and predict that the Z boson cannot decay to any two  $n = 0$  particles. As the Z boson is known to decay to neutrino-antineutrino pairs, it follows that the neutrino is *not* an  $n = 0$  particle, and therefore that the neutrino is *not* a majorana particle (as majorana particles are their own antiparticles, and should have  $n = 0$ ).

We next consider the decay of a particle with spin  $S_i$  and  $n = \sqrt{S_i(S_i + 1)}$ . We require that the projection of  $\mathbf{S}$  along the  $z'$  axis, and the subsequent projection on the Z axis (or any space-fixed axis) between initial particles and the final particles must be conserved, given by  $|\mathbf{S}| \langle \cos\theta \rangle$ :

$$\frac{n_i M_i}{\sqrt{S_i(S_i + 1)}} = \sum_f \frac{n_f M_f}{\sqrt{S_f(S_f + 1)}} \quad (41)$$

where  $\langle \cos\theta \rangle = nM/S(S + 1)$  from Eq. 18b, and  $|\mathbf{S}| = \sqrt{S(S + 1)}$ .

For example, we consider the decay of a  $W^+$  boson in the  $|SM\rangle = |11\rangle$  state into a positron and an electron neutrino ( $W^+ \rightarrow e^+ + \nu_e$ ):

$$\frac{n_{W^+} M_{W^+}}{\sqrt{S_{W^+}(S_{W^+} + 1)}} = \frac{n_{e^+} M_{e^+}}{\sqrt{S_{e^+}(S_{e^+} + 1)}} + \frac{n_{\nu_e} M_{\nu_e}}{\sqrt{S_{\nu_e}(S_{\nu_e} + 1)}} \quad (42a)$$

where  $S_{W^+} = M_{W^+} = 1$ ,  $S_{e^+} = M_{e^+} = \frac{1}{2}$ ,  $S_{\nu_e} = M_{\nu_e} = \frac{1}{2}$ ,  $n_{W^+} = \sqrt{S_{W^+}(S_{W^+} + 1)} = \sqrt{2}$ ,  $n_{e^+} = \sqrt{S_{e^+}(S_{e^+} + 1)} = \sqrt{3}/2$ , and note that  $M_{W^+} = M_{e^+} + M_{\nu_e}$ . Inserting these values into Eq. (42a) gives:

$$1 = \frac{1}{2} + \frac{1}{2} \left( \frac{n_{\nu_e}}{\sqrt{S_{\nu_e}(S_{\nu_e} + 1)}} \right) \quad (42b)$$

and therefore that  $n_{\nu_e} = \sqrt{S_{\nu_e}(S_{\nu_e} + 1)} = \sqrt{3}/2$ . Thus, we determine that the neutrino has the same internal projection as charged fermions. Therefore, we determine again, from a different reaction, that

the neutrino is a Dirac fermion and not a Majorana fermion [28], as it is *not* its own antiparticle (which could only be the case for  $n_{\nu_e} = 0$ ), and its spin wavefunction is described by  $D_{nm}^{\frac{1}{2}}(\varphi, \theta, \chi)$  with  $n = \sqrt{3}/2$ .

## VIII. DARK MATTER CANDIDATES

Baryonic matter is associated with at least three obvious asymmetries: (1) the preponderance of matter over antimatter; (2) the fact that known baryonic matter violates parity through the weak interaction; and (3) the further asymmetry introduced here, that known baryons have internal angular momentum projection  $n = \sqrt{S(S+1)}$  only, which constitutes a lack of isotropy in the internal (body-fixed) coordinate system (due to lack of baryons with  $n = 0$ , needed for isotropy in the internal coordinate system).

Mirror Matter [29] has been proposed as a solution to asymmetry (2), which results in a doubling of all Standard Model particles with mirror pairs, that are dark with respect to normal baryonic matter, and have opposite parity violation effects. However, Mirror Matter particles will be as self-interacting as normal baryonic matter is, and so can only constitute a small fraction of the dark matter, as the  $\Lambda$ CDM model assumes non-interacting dark matter, and it explains the cosmic background radiation power spectrum well [30]. Nevertheless, there is evidence that suggests the existence of some self-interacting dark matter [31,32,33,34], and Mirror Matter offers a plausible explanation for such self-interacting dark matter.

We address the lack of isotropy of asymmetry (3) by proposing that there exists neutral baryonic matter, based on neutral quarks that have internal projection  $n = 0$ , and with similar mass as charged baryonic matter; we also address the parity asymmetry (2) by proposing equal amounts of mirror matter; finally, we can also address the matter-antimatter asymmetry (1) by proposing that the mirror matter is also antimatter. In this way, all three symmetries are addressed, albeit symmetries (1) and (2) are entangled; however, it seems that this is the highest symmetry for which the matter and antimatter does not annihilate.

The abundance particles of the proposed symmetries is shown in Fig. 5. There are 6 equal parts: 1/6 of baryonic matter, 1/6 of antimirror matter, 2/6 of baryonic dark matter, and 2/6 of anti-mirror dark matter (note that the antimirror matter is dark to the baryonic matter). Therefore, the predicted fraction that is dark matter is 5/6, which agrees well with experimental observations of 85% [30]. We note that if the mass of the ( $n = 0$ ) neutral quarks are larger than the charged quarks, by a similar ratio as that of the ( $n = 0$ ) Z boson to the W boson (by about 1.13), then the calculated dark matter fraction increases from

5/6 to 85%, to give exact agreement.

We now consider whether these neutral ( $n = 0$ ) baryons can be observed directly, either through direct decay, or produced at particle colliders. First, they cannot decay to any known Standard-Model particles,

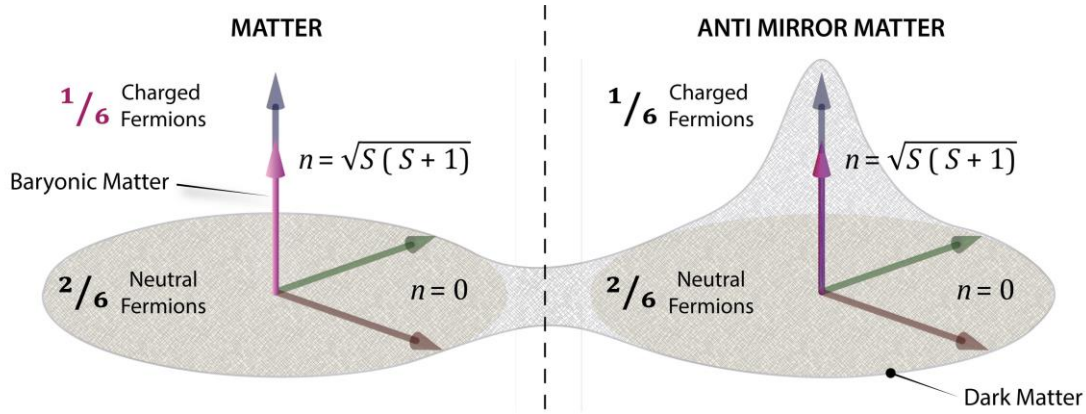


*Figure 5: The proposed abundance of particles: 1/6 is baryonic matter, and the remaining 5/6 is dark matter. Of the 5/6 dark matter, 1/6 is antimirror matter, 2/6 baryonic dark matter, and 2/6 of anti-mirror dark matter; therefore, 4/6 of the dark matter is cold dark matter (CDM), and 1/6 (the antimirror matter) is self-interacting.*

because it is not possible to do so while conserving charge, lepton number, and baryon number. Second, we showed, using Eq. (37), that the decay of a Z boson is forbidden to any  $n = 0$  particle-antiparticle pair (such as two photons or two neutral quarks); this explains why neutral quarks cannot be formed from Z boson decay. Third, a channel for potentially observing evidence for these dark-matter particles is the formation of neutral quark-antiquark pairs from the decay of the Higgs boson. Current searches for dark channels limit their fraction to about 18% ( $2\sigma = 10\%$ ) [35]. A calculation of the expected production of neutral quark-antiquark pairs can be compared to this dark-channel uncertainty, to test this possibility; furthermore, future experiments will reduce the dark-channel uncertainty further.

An additional prediction that can be tested, is that the self-interacting Mirror Matter is 1/6 of the total matter (from Fig. X, equal to the baryonic contribution). It can be investigated whether the tension in the current dark-matter models is eliminated or reduced from the inclusion of the self-interacting Mirror Matter (1/5 of the total dark matter).

## IX. INTERNAL PROJECTIONS FOR THE STRONG AND WEAK FORCES

In this paper, we have proposed that the spin of fundamental particles have three internal projections, described by  $n_{x'} = n_{y'} = n_{z'} = \sqrt{j(j+1)}$  (or equivalently,  $n_{z'} = \sqrt{j(j+1)}$  and the doubly degenerate  $n_{z'} = 0$ ). Spin is associated with the electromagnetic force; there are very close analogues of spin for the strong and weak forces (isospin and weak isospin, respectively), and it is natural to consider whether the three internal projections also exist for these forces. We propose that they do, and that they are already clearly present in the Standard Model: the three internal projections are the three quark colors (for the spin associated with strong force) and the three generations of matter (for weak

isospin). We present the similar projection structure for the three forces in Fig. 6, to highlight the similarities and the differences.

For the electromagnetic force, one projection of the spin is fully parallel to the charge field, so that the particles of this state have charge  $q=1$  (in units of  $e$ ); in contrast, the other two orthogonal states have 0 projection on the charge field, and thus are neutral (these correspond to dark matter; see section VIII

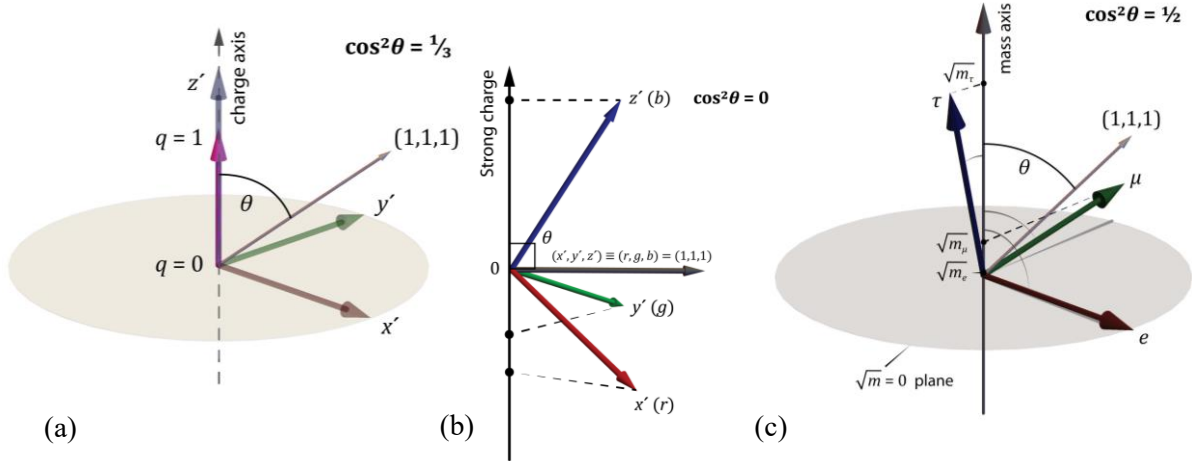


**Figure 6:** The three spin-projection states in the (a) electromagnetic, (b) strong, and (c) weak forces. See text for details. and Fig. 5).

For the strong force, each of the three spin projections correspond to the three colors of quarks. The (1,1,1) vector, which corresponds to the sum of all three projection vectors, is perpendicular to the strong-charge axis. The arrangement of the three states is such that each state has an irrational projection on the charge field, and thus has an irrational charge, which is forbidden, as it must be quantized for each free particle. However, either a quark-antiquark pair or three quarks of each projection (color) yields zero projection, and hence a zero net strong charge, which is quantized and allowed. Therefore, Fig. 6b gives a geometric interpretation of the known rules for quark combinations, to yield a colorless combination for allowed composite particles.

For the weak force, we propose that the internal weak isospin projections play a role in determining the particle mass of the fermions, and thus these three projections produce the three generations of matter (for the quarks and the leptons). For the charged leptons, these three projections correspond to the electron, muon, and tau. Koide noticed in 1981 that the masses of the charged leptons are related by a simple formula [36]:

$$\frac{m_e + m_\mu + m_\tau}{(\sqrt{m_e} + \sqrt{m_\mu} + \sqrt{m_\tau})^2} = \frac{2}{3} \quad (43)$$

A geometric interpretation of Eq. (43) was proposed by Foot [37], that the (1,1,1) vector is at an angle of  $45^\circ$  to the mass axis. This interpretation, shown in Fig. 6c, is consistent with the space of the three internal spin projections.

In general, we see that the internal projections seem to play a similar role in all three forces, in

determining the charge or mass of particles, but the character of the symmetry breaking is different for each of them, with the square of the cosine of the angle between the (1,1,1) vector and the charge/mass axis (shown in Fig. 6a, 6b, and 6c) being 1/3, 0, and 1/2, respectively. In our opinion, this similarity makes the argument for the existence of dark matter more compelling.

## X. CONCLUSIONS

We have presented the angular momentum spatial wavefunctions  $D_{nm}^j(\varphi, \theta, \chi)$ , that treat  $j$  as a three dimensional entity. Compared to the conventional  $|jm\rangle$  states, these wavefunctions have an additional body-fixed spin projection:  $n = \sqrt{j(j+1)}$  or  $n = 0$ . For  $n = \sqrt{l(l+1)}$ , these wavefunctions describe orbital angular momentum  $\mathbf{l}$ , and in the high- $l$  limit, they connect with the semiclassical wavefunction of Eq. (1). Therefore, a seamless connection is provided between quantum, semiclassical, and classical angular momentum. Furthermore, we show that the  $D_{\sqrt{S(S+1)}M}^S(\varphi, \theta, \chi)$  spatial wavefunctions of the spin of charged fundamental particles give with gyromagnetic ratios of  $g = 2$  at the tree level, therefore we propose that the  $D_{\sqrt{S(S+1)}M}^S(\varphi, \theta, \chi)$  are spatial wavefunctions of the charged elementary particles (e.g. electron, muon, tau, quarks, and W boson). States with internal projection  $n = 0$  correspond to the remaining neutral particles (photon, gluon, and Z boson), and we also propose a dark matter candidate with this projection. In addition, using the selection rule of Eq. (40) and internal-projection conservation of Eq. (42), we show that the neutrino is described by  $n = \sqrt{S(S+1)}$ , and is thus a Dirac fermion.

The advantage of our concept of a spatial wavefunction for spin is that it can reproduce all known angular-momentum theory, while at the same time, it can go a little further: the new internal projection  $n$  allows the seamless connection of quantum-mechanical and classical angular momentum [10]; and it allows us to make testable predictions or hypotheses that go beyond standard angular-momentum theory (e.g. the Dirac-fermion nature of the neutrino, some decay selection rules of fundamental particles, and the prediction of properties of new dark-matter candidates). Most importantly, these predictions are expected to be tested in the next few years, as there are intensive experimental efforts related to all three predictions.

This work was partially supported by the Hellenic Foundation for Research and Innovation (HFRI) and the General Secretariat for Research and Technology (GSRT), under grant agreement No. HFRI-FM17-3709 (project NUPOL). We thank Giorgos Katsoprinakis for assistance with the figures, and Vasilis Niarchos for making helpful suggestions.

## APPENDIX A

Here we show that, for all  $n$ :

$$\hat{J}_- \hat{J}_+ D_{n,j}^j(\varphi, \theta, \chi) = 0 \quad (\text{A1})$$

$D_{n,j}^j(\varphi, \theta, \chi)$  is defined in Eq. (5), and  $d_{n,j}^j(\theta)$  is given in Eq. (10), where there are two terms, proportional to the constants  $A$  and  $B$ . For the first term, for  $m = j$ ,  ${}_2F_1\left(m - j, m + j + 1; 1 + m - n; \sin^2 \frac{\theta}{2}\right) = 1$ , so that the first term reduces to  $A e^{ij\varphi} \left(\sin \frac{\theta}{2}\right)^{j-n} \left(\cos \frac{\theta}{2}\right)^{j+n} e^{in\chi}$ . Operation of  $\hat{J}_+$  on this term, from Eq. (12), gives 0, satisfying Eq. (A1) for all  $n$ . Operation of  $\hat{J}_+$  on the second term yields:

$$\begin{aligned} \hat{J}_+ B \left(\sin \frac{\theta}{2}\right)^{n-j} \left(\cos \frac{\theta}{2}\right)^{n+j} {}_2F_1\left(n - j, n + j + 1; 1 + n - j; \sin^2 \frac{\theta}{2}\right) \\ = B e^{i(j+1)\varphi} (n - j) \left(\sin \frac{\theta}{2}\right)^{-j+n-1} \left(\cos \frac{\theta}{2}\right)^{-j-n-1} e^{in\chi} \end{aligned} \quad (\text{A2})$$

Finally, the operation of  $\hat{J}_-$  on the result of Eq. (A2) yields 0, showing that Eq. (A1) holds for all  $n$ , and by symmetry,  $\hat{J}_+ \hat{J}_- D_{n,-j}^j(\varphi, \theta, \chi) = 0$ .

## APPENDIX B

We demonstrate the use of Eq. (19) by calculating the expectation value  $\cos \theta$  for  $|\Psi\rangle = D_{1, \frac{1}{2}}^{\frac{1}{2}}(\theta)$ . First, we calculate the norm, from Eq. (19a):

$$\Psi^* \Psi \sin \theta = \frac{|N_{1/2}|^2}{2} \left[ 2 \left(\cos \frac{\theta}{2}\right)^4 + \frac{1}{2} \left(\cos \frac{\theta}{2}\right)^{-2} \left(\sin \frac{\theta}{2}\right)^2 (2 + \cos \theta)^2 \right] \quad (\text{B1})$$

Then, we expand the second term (which diverges at  $\theta = \pi$ ), in powers of  $\sin \theta$ :

$$\begin{aligned} \frac{1}{2} \left(\cos \frac{\theta}{2}\right)^{-2} \left(\sin \frac{\theta}{2}\right)^2 (2 + \cos \theta)^2 &= \frac{\left(\sin \frac{\theta}{2}\right)^4 (2 + \cos \theta)^2}{2 \left(\sin \frac{\theta}{2}\right)^2 \left(\cos \frac{\theta}{2}\right)^2} = \frac{(1 - \cos \theta)^2 (2 + \cos \theta)^2}{2 \sin^2 \theta} \\ &= \frac{1 - \cos \theta}{\sin^2 \theta} + \frac{1 - 2 \cos \theta + \sin^2 \theta}{2} \end{aligned} \quad (\text{B2})$$

Using Eq. (19b), we subtract off the diverging first term (where  $f(\theta) = (1 - \cos \theta) / \sin^2 \theta$ ), and then express in terms of  $\cos \frac{\theta}{2}$  as :

$$\frac{1}{2} \left(\cos \frac{\theta}{2}\right)^{-2} \left(\sin \frac{\theta}{2}\right)^2 (2 + \cos \theta)^2 - f(\theta) = \frac{3}{2} - 2 \left(\cos \frac{\theta}{2}\right)^4 \quad (\text{B3})$$

After this regularization, Eq. (B3) can be written as:

$$\Psi^* \Psi \sin \theta - f(\theta) = \frac{|N_{1/2}|^2}{2} \left[ 2 \left( \cos \frac{\theta}{2} \right)^4 + \frac{3}{2} - 2 \left( \cos \frac{\theta}{2} \right)^4 \right] = \frac{3}{4} |N_{1/2}|^2 \quad (\text{B4})$$

Notice that, through this renormalization procedure, the dependence on the angle  $\theta$  cancels, leaving only a constant term.

Finally, we perform the integral of Eq. (19a) on the result of (B4) to yield

$$\int_0^\pi d\theta \left[ \sin \theta \int_0^{2\pi} d\varphi \Psi^*(\varphi, \theta, \chi) \cos \theta \Psi'(\varphi, \theta, \chi) - f(\theta) \right] = \frac{3}{2} \pi^2 |N_{1/2}|^2 \quad (\text{B5})$$

We now follow a similar procedure for the calculation of  $\langle \Psi | \cos \theta | \Psi \rangle$ :

$$\Psi^* \cos \theta \Psi \sin \theta = \frac{|N_{1/2}|^2}{2} \cos \theta \left[ 2 \left( \cos \frac{\theta}{2} \right)^4 + \frac{1}{2} \left( \cos \frac{\theta}{2} \right)^{-2} \left( \sin \frac{\theta}{2} \right)^2 (2 + \cos \theta)^2 \right] \quad (\text{B6})$$

Then, we expand the second term (which diverges at  $\theta = \pi$ ), in powers of  $\sin \theta$ :

$$\begin{aligned} \frac{\cos \theta}{2} \left( \cos \frac{\theta}{2} \right)^{-2} \left( \sin \frac{\theta}{2} \right)^2 (2 + \cos \theta)^2 &= \frac{\cos \theta (1 - \cos \theta)^2 (2 + \cos \theta)^2}{2 \sin^2 \theta} \\ &= \frac{-1 + \cos \theta}{\sin^2 \theta} + \frac{\cos \theta + 2 \sin^2 \theta + \cos \theta \sin^2 \theta}{2} \end{aligned} \quad (\text{B7})$$

Combining the first term with the renormalized second term, and integrating gives:

$$\begin{aligned} &|N_{1/2}|^2 \int_0^\pi d\theta \left[ \sin \theta \int_0^{2\pi} d\varphi \left( \sin \theta \cos \theta \left( \cos \frac{\theta}{2} \right)^4 + \frac{\cos \theta + 2 \sin^2 \theta + \cos \theta \sin^2 \theta}{4} \right) \right] \\ &= \pi^2 |N_{1/2}|^2 \end{aligned} \quad (\text{B8})$$

Finally, the expectation value  $\cos \theta$  for  $|\Psi\rangle = D_{1/2}^{\frac{1}{2}}(\theta)$  is given by the ratio of the results of the integrals of Eqs. (B5) and (B8), which is  $\langle \cos \theta \rangle = 2/3$ . This agrees with  $\langle \cos \theta \rangle = nM/S(S+1)$ , the analytical result from Eq. (21b), for  $S = M = 1/2$  and  $n = 1$ .

## REFERENCES

---

- [1] D. J. Griffiths, "Introduction to Quantum Mechanics," 2nd Edition, Pearson Prentice Hall, Upper Saddle River, New Jersey, 2005.
- [2] S. E. Choi and R. B. Bernstein, "Theory of oriented symmetric-top molecule beams: Precession, degree of orientation, and photofragmentation of rotationally state-selected molecules", *J. Chem. Phys.* **85**, 150 (1986), DOI: [10.1063/1.451821](https://doi.org/10.1063/1.451821)
- [3] R.D. Levine, R.B. Bernstein, "Rotational state dependence of the reactivity of oriented symmetric top molecules", *Chem. Phys. Lett.* **132**, 11 (1986). DOI: [10.1016/0009-2614\(86\)80685-6](https://doi.org/10.1016/0009-2614(86)80685-6)
- [4] R. N. Zare, "Photofragment angular distributions from oriented symmetric-top precursor molecules", *Chem. Phys. Lett.* **156**, 1 (1989), DOI: [10.1016/0009-2614\(89\)87070-8](https://doi.org/10.1016/0009-2614(89)87070-8)
- [5] Suketu R. Gandhi, Thomas J. Curtiss, Qi-Xun Xu, Seung E. Choi, Richard B. Bernstein, "Oriented molecule beams: pulsed, focused beams of methyl halides in pure JKM rotational states", *Chem. Phys. Lett.* **132**, 6 (1986), DOI: [10.1016/0009-2614\(86\)80684-4](https://doi.org/10.1016/0009-2614(86)80684-4)
- [6] E. W. Kuipers, M. G. Tenner, A. W. Kleyn & S. Stolte, "Observation of steric effects in gas-surface scattering", *Nature* **334**, 420 (1988), DOI: [10.1038/334420a0](https://doi.org/10.1038/334420a0)
- [7] T.P. Rakitzis, A.J. van den Brom, M.H.M. Janssen, "Directional dynamics in photodissociation of oriented molecules", *Science* **303**, 1852 (2004), DOI: [10.1126/science.1094186](https://doi.org/10.1126/science.1094186)
- [8] F. Wang, K. Liu, & T. P. Rakitzis, "Revealing the stereospecific chemistry of the reaction of Cl with aligned  $\text{CHD}_3(v_1 = 1)$ ", *Nature Chem.* **4**, 636 (2012), DOI: [10.1038/nchem.1383](https://doi.org/10.1038/nchem.1383)
- [9] D. Pandres and D. A. Jacobson, "Scalar Product for Harmonic Functions of the Group  $\text{SU}(2)$ ", *J. Math. Phys.* **9**, 1401 (1968).
- [10] T. P. Rakitzis, M. E. Koutrakis, G. E. Katsoprinakis, "The "Vector-Model" Wavefunction: spatial description and wavepacket formation of quantum-mechanical angular momenta", [arXiv:2305.11456v2](https://arxiv.org/abs/2305.11456v2), 2023.
- [11] S. Ferrara, M. Porrati, V. L. Telegdi, " $g=2$  as the natural value of the tree-level gyromagnetic ratio of elementary particles", CERN-TH.6432/92 UCLA/92/TEP/7, 1992, DOI: [10.1103/PhysRevD.46.3529](https://doi.org/10.1103/PhysRevD.46.3529)
- [12] B. R. Holstein, "How Large is the "Natural" Magnetic Moment?", *Am. J. Phys.* **74**, 1104-1111 (2006), DOI: [10.1119/1.2345655](https://doi.org/10.1119/1.2345655)
- [13] R. N. Zare, "*Angular Momentum*", Wiley, New York, 1988, ISBN: 978-0-471-85892-8
- [14] R. N. Zare, "*Angular Momentum*", Wiley, New York, 1988, ISBN: 978-0-471-85892-8
- [15] D. Pandres, "Schrodinger Basis for Spinor Representations of the Three-Dimensional Rotation Group", *J. Math. Phys.* **6**, 1098 (1965).
- [16] M. Pavsic, "Rigid Particle and its Spin Revisited" *Found. Phys.* **37**, 40 (2007), DOI: [10.1007/s10701-006-9094-4](https://doi.org/10.1007/s10701-006-9094-4)
- [17] J. J. Sakurai, "*Advanced Quantum Mechanics*", Addison-Wesley, 1967, ISBN: 9780201067101
- [18] A. R. Edmonds, "*Angular Momentum in Quantum Mechanics*", Princeton University Press, 1974, ISBN: 9780691025896
- [19] S. Weinberg, "*The Quantum Theory of Fields, Volume 1: Foundations*" Cambridge University Press, 2005, ISBN: 9781139644167.
- [20] J.-M. Levy-Leblond, "Nonrelativistic particles and wave equations", *Commun. Math. Phys.*, **6**, 286-311

---

(1967), DOI: [10.1007/BF01646020](https://doi.org/10.1007/BF01646020)

[21] J.D. Bjorken and S.D. Drell, “Relativistic Quantum Mechanics”, McGraw-Hill, New York (1964)

[22] A. Proca, “Sur les Equations Fondamentales des Particules Elementaires,” *Comp. Ren. Acad. Sci. Paris* **202**, 1366 (1936).

[23] F.J. Belinfante, “Intrinsic Magnetic Moment of Elementary Particles of Spin 3/2,” *Phys. Rev.* **92**, 997 (1953), DOI: [10.1103/PhysRev.92.997](https://doi.org/10.1103/PhysRev.92.997)

[24] Particle Data Group, S. Eidelman et al., “Review of Particle Physics”, *Phys. Lett.* **B592**, 1 (2004), DOI: [10.1016/j.physletb.2004.06.001](https://doi.org/10.1016/j.physletb.2004.06.001)

[25] I.J.R. Aitchison and A.J.G. Hey, “Gauge Theories in Particle Physics”, Adam Hilger, Philadelphia (1989), ISBN: 0-85274-329-7

[26] L. D. Landau, "The moment of a 2-photon system", *Dokl. Akad. Nauk SSSR.* **60**, 207 (1948).

[27] C. N. Yang, "Selection Rules for the Dematerialization of a Particle into Two Photons", *Phys. Rev.* **77**, 242 (1950), DOI:[10.1103/PhysRev.77.242](https://doi.org/10.1103/PhysRev.77.242)

[28] A. Baha Balantekin and Boris Kayser, “On the Properties of Neutrinos” *Annu. Rev. Nucl.* **68** 313 (2018), DOI: [10.1146/annurev-nucl-101916-123044](https://doi.org/10.1146/annurev-nucl-101916-123044)

[29] R. Foot, “Mirror Matter-Type Dark Matter”, *Int. J. Mod. Phys. D* **13**, 2161 (2004), DOI: [10.1142/S0218271804006449](https://doi.org/10.1142/S0218271804006449)

[30] Ade et al. (Planck Collaboration), “Planck 2013 results. XVI. Cosmological parameters”,*A&A* **571**, A16 (2014), DOI: [10.1051/0004-6361/201321591](https://doi.org/10.1051/0004-6361/201321591)

[31] J. S. Bullock and M. Boylan-Kolchin, , *Ann. Rev. Astron. Astrophys.*, **55**, 343 (2017), DOI: [10.1146/annurev-astro-091916-055313](https://doi.org/10.1146/annurev-astro-091916-055313)

[32] F. Governato et al., “Bulgeless dwarf galaxies and dark matter cores from supernova-driven outflows”, *Nature* **463**, 203 (2010), DOI: [10.1038/nature08640](https://doi.org/10.1038/nature08640)

[33] N. C. Relatores et al., “The Dark Matter Distributions in Low-mass Disk Galaxies. II. The Inner Density Profiles”, *ApJ* **887**, 94 (2019), DOI: [10.3847/1538-4357/ab5305](https://doi.org/10.3847/1538-4357/ab5305)

[34] Ethan O. Nadler et al., “A Self-interacting Dark Matter Solution to the Extreme Diversity of Low-mass Halo Properties”, *ApJL* **958**, L39 (2023), DOI: [10.3847/2041-8213/ad0e09](https://doi.org/10.3847/2041-8213/ad0e09)

[35] A. Tumasyan et al. (CMS Collaboration) *Phys. Rev. D* **105**, 092007 (2022), DOI: [10.1103/PhysRevD.105.092007](https://doi.org/10.1103/PhysRevD.105.092007)

[36] Y. Koide, “A New Formula For The Cabibbo Angle And Composite Quarks And Leptons,” *Phys. Rev. Lett.* **47**, 1241 (1981).

[37] R. Foot, arXiv:hep-ph/9402242 (1994).